

Article

A Numerical Study on Dust Control: Evaluating the Impact of Spray Angle and Airflow Speed in the Coalescence of Droplets and Dust

Jinming Mo

CCTEG Chongqing Research Institute, Chongqing 400037, China; jinmingmo_ccteg@163.com;
Tel.: +86-133-1233-2468

Abstract: Spray dust reduction is one of the most economical and effective technologies for controlling coal dust in coal mining faces. We aimed to reproduce a spray dust reduction process in a simulation and investigate the mechanism by which the spray angle and airflow speed influence the dust reduction effect. Based on the DPM (discrete phase model) and the mixture model, we constructed a spray dust reduction evaluation model by considering two-way momentum coupling between the discrete phase and the continuous phase. The results showed that installing nozzles near the dust source (coal mining drum) significantly reduced the dust concentration at the coal mining face from 0.0005 kg/m^3 to 0.0001 kg/m^3 . The increase in airflow speed and spray angle enhanced the horizontal transportation of droplets and dust, providing opportunities for the droplets to condense the dust; however, if the droplets have too large an angle, this will result in an insufficient concentration of droplets in the vicinity of the dust source. When the spray angle is 45° , increasing the airflow speed provides a better dust reduction effect. The nozzle position should also be set scientifically according to the airflow speed. Based on simulation results, a mathematical calculation model of spray dust reduction efficiency was constructed. These results can guide the key parameters of spray dust reduction systems, such as the installation position of the nozzle, the spray angle, and the airflow speed. This paper provides ideas for simulating spray dust reduction for other dust types.

Keywords: spray dust reduction; droplet distribution; coal dust distribution; spray angle; airflow speed; dust reduction simulation



Citation: Mo, J. A Numerical Study on Dust Control: Evaluating the Impact of Spray Angle and Airflow Speed in the Coalescence of Droplets and Dust. *Processes* **2024**, *12*, 937. <https://doi.org/10.3390/pr12050937>

Received: 28 March 2024
Revised: 26 April 2024
Accepted: 28 April 2024
Published: 4 May 2024



Copyright: © 2024 by the author. Licensee MDPI, Basel, Switzerland. This article is an open access article distributed under the terms and conditions of the Creative Commons Attribution (CC BY) license (<https://creativecommons.org/licenses/by/4.0/>).

1. Introduction

Coal dust generated during coal mining threatens the health of coal miners [1,2]. In addition, it may cause serious accidents such as explosions [3], which brings great challenges to coal mine production and management. To solve the problem of coal dust in coal mines, researchers continue to explore and gradually develop spray dust reduction technology [4]. The mature and environmentally friendly characteristics of spray dust reduction technology have gradually made this an important means of dust reduction in coal mines. This technology first atomizes liquid into tiny water droplets, which are transported onto airborne dust particles and then co-settled on the ground, thus reducing the concentration of dust in the air and improving the working environment.

There are two main types of spraying used for dust reduction: internal spraying and external spraying. Internal spraying involves spraying near the drum of the coal mining machine to control the dust from its source [5]. External spraying is when a spray field forms around a coal mining drum and droplets are then used to capture coal dust particles [6]. Solution properties [7–9], nozzle size [10], spray pressure [11], and airflow conditions [12] are important factors in the effectiveness of spray dust reduction, for which scholars have carried out a large number of studies. Zhou et al. [13] investigated the effect of spray pressure and nozzle caliber on the atomization of the spray, and the results showed that the atomization effect of the spray was best when the nozzle diameter was 1.5 mm and

the spray pressure was 5 MPa. Klima et al. [14] developed a movable water curtain near a coal mining machine and provided the optimal spray parameters for the experimental conditions (a spray angle of 75° and a spray distance of 1.37 m). Ren et al. [15] investigated the distribution law of the spray field, extending the direction of airflow, based on which a new dust removal spray system was developed. To achieve better spray atomization, some scholars have used water and air synergistic spraying [16], where the sprayed air causes the droplets to be broken up twice, further enhancing the turbulence of the sprayed liquid [17]. The dust control efficiency of air–water spray is more than 30% higher than that of ordinary water spray, and its water consumption is 30% lower than that of ordinary water mist [18]. Dominik developed a novel dust control device based on air–water spray and found an average effectiveness of more than 60% in reducing PM10 and PM2.5 dust [19].

Owing to the complexity of coal mining faces, physically similar experiments on the ground are costly and difficult to carry out. Establishing an effective numerical calculation model can guide the design of spraying and dust reduction systems in coal mining faces. Previous studies have focused on numerical simulation studies of airflow–droplet fields and airflow–dust fields. Lee et al. [20] determined the three-dimensional velocity of droplets produced by a conical atomizing nozzle and the evolution of droplet size through numerical simulation. Zhou Gang et al. [21] simulated an airflow–droplet field and an airflow–dust field in a coal mining face and successfully provided scientific guidance for a spray dust reduction system.

However, as noted, these numerical simulation studies have generally focused on airflow–droplet fields and airflow–dust fields and lack reproductions of droplet–dust coagulation and the deposition process. Therefore, using Ansys Fluent software (2022) [22], this study focuses on the dust reduction process by spraying at a coal mining face, establishes a numerical model of airflow–droplet–dust three-field coupling, and systematically researches the effect of different airflow speeds and spraying angles on dust reduction using a spraying system. These results can guide the design of spray dust reduction systems in coal mining faces, which is of great practical significance.

2. Numerical Approach

2.1. Mathematical Model

Gas is defined as a continuous medium and can be described by the Eulerian method. Spray particles are defined as a discrete medium and tracked in their lanes using the Lagrangian method. Dust and droplets can be described by the mixture (mixture model) and the DPM (discrete phase model), respectively. In the mixture model, the primary phase is air, and the secondary phase is dust. Our simulation concept is shown in Figure 1.

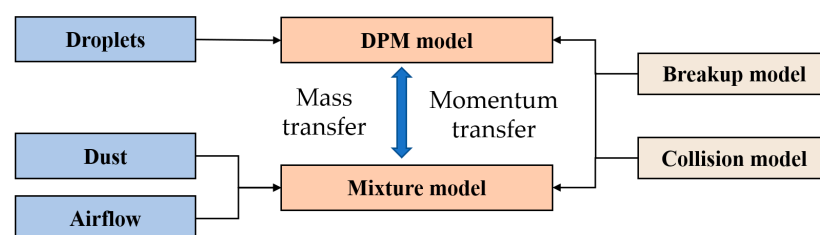


Figure 1. Simulation flowchart.

2.1.1. Conservation Equation

The continuity, momentum, and energy equations are as follows:

$$\frac{\partial}{\partial t}(\rho_m) + \nabla \cdot (\rho_m \vec{V}_m) = 0 \quad (1)$$

$$\frac{\partial}{\partial t}(\rho_m \vec{V}_m) + \nabla \cdot (\rho_m \vec{V}_m \vec{V}_m) = -\nabla p + \nabla \cdot [\mu_m(\nabla \vec{V}_m + \nabla \vec{V}_m^T)] + \rho_m \vec{g} + \vec{F} - \nabla \cdot \left(\sum_{k=1}^n \alpha_k \rho_k \vec{V}_{dr,k} \vec{V}_{dr,k} \right) \quad (2)$$

$$\frac{\partial}{\partial t} \sum_k \alpha_k \rho_k E_k + \nabla \cdot \sum_k (\alpha_k \vec{V}_k (\rho_k E_k + p)) = \nabla \cdot (k_{eff} \nabla T - \sum_k \sum_j h_{j,k} \vec{J}_{j,k} + (\bar{\tau}_{eff} \cdot \vec{V})) + s_h \quad (3)$$

where ρ_m is the mixture density; \vec{V}_m is the mass-averaged velocity; n is the number of phases; \vec{F} is a body force; μ_m is the viscosity of the mixture; $\vec{V}_{dr,k}$ is the drift velocity for the secondary phase; $h_{j,k}$ is the enthalpy of species in the phase; $\vec{J}_{j,k}$ is the diffusive flux of species in the phase; and k_{eff} is the effective conductivity.

The force balance of the tracked particles in the calculated flow field in the Lagrangian coordinate system can predict a particle's movement pattern, which can be expressed as follows:

$$m_p \frac{d\vec{u}_p}{dt} = m_p \frac{\vec{u} - \vec{u}_p}{\tau_r} + m_p \frac{g(\rho_p - \rho)}{\rho_p} + \vec{F} \quad (4)$$

where m_p is the particle mass; u is the fluid phase velocity; u_p is the particle velocity; ρ is the fluid density; ρ_p is the particle density; \vec{F} is the additional force; $m_p \frac{\vec{u} - \vec{u}_p}{\tau_r}$ is the drag force; and τ is the relaxation time of the droplet.

2.1.2. Collision Model

According to the O'Rourke model [23], the collision probability of two droplets is calculated from the perspective of the larger droplet. Relatively speaking, the larger droplet has zero velocity, and its collision probability mainly depends on the relative distance between the larger droplet and the smaller droplet and the trajectory of the smaller droplet. The collision probability can be described as follows:

$$P_1 = \frac{\pi(r_1 + r_2)^2 v_{rel} \Delta t}{V} \quad (5)$$

where P_1 is the probability of collision between a large droplet and a small droplet; V is the volume of the cell in the continuous phase where the small droplet is located; r_1 is the radius of the large droplet; r_2 is the radius of the small droplet; v_{rel} is the velocity of the small droplet; and Δt is the time step.

2.1.3. Breakup Model

The amplitude of the undamped oscillations of each droplet is first determined and denoted as:

$$A = \sqrt{(y^n - We_c)^2 + \left(\frac{(dy)/dt}{\omega}\right)^2} \quad (6)$$

$$We_c = \frac{C_F}{C_k C_b} We \quad (7)$$

$$y = x / (C_b r) \quad (8)$$

where x is the displacement; ω is the droplet oscillation frequency; and C_F , C_k , and C_b are the three dimensionless numbers, 8, 5, and 1/3, respectively.

The droplet breaks up when $We_c + A > 1$.

2.1.4. Coupling between Discrete and Continuous Phases

The momentum transfer from the continuous phase to the discrete phase can be computed in the Ansys Fluent model by examining the change in momentum of a particle as it passes through each control volume. This momentum change can be computed as:

$$F = \sum \left(\frac{18\mu C_D Re}{\rho_p d_p^2 24} (u_p - u) + F_{other} \right) \dot{m}_p \Delta t \quad (9)$$

where u is the viscosity of the fluid; ρ_p is the density of the particle; d_p is the diameter of the particle; C_D is the drag coefficient; Re is the relative Reynolds number; u_p is the velocity of the particle; and \dot{m}_p is the mass flow rate.

The mass transfer from the discrete phase to the continuous phase is computed in the Ansys Fluent model by examining the change in mass of a particle as it passes through each control volume. The mass change can be computed simply as:

$$M = \frac{\Delta m_p}{m_{p,0}} \dot{m}_{p,0} \quad (10)$$

where $\dot{m}_{p,0}$ is the initial mass flow rate of the particle injection and $m_{p,0}$ is the initial mass of the particle.

2.2. Simulation Setup

To study the distribution of droplets in a coal mining face, we modeled the dimensions of a real coal mining face, but ignored obstacles other than the coal mining machine and hydraulic pillars. Figure 2 shows that the total length of the geometric model is 50 m, the height is 7 m, and it is divided into 1,996,587 meshes by the ICEM software (2022). Three water mist nozzles were set near the front and rear drums of the coal mining machine at intervals of 1.5 m, a nozzle diameter of 0.0015 m, a spray half angle of 30° , and a spray pressure of 3 MPa. The pressure, temperature, and humidity parameters of the coal mining face affect the efficiency of spray dust reduction. However, compared with the spray angle and airflow speed, these parameters have less influence on the dust reduction efficiency of the spray, so this study focuses on the influence of the spray angle and airflow speed on dust reduction efficiency.

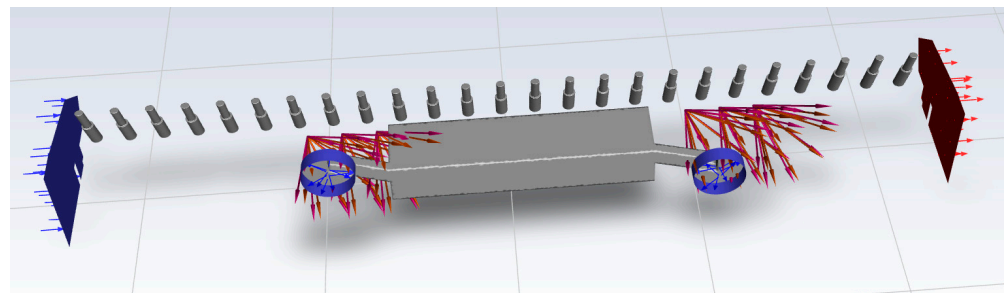


Figure 2. Geometric model of the coal mining face.

In the numerical model, the droplets are treated as discrete phases, and the dust and air are treated as mixed phases, where the air is the main phase, coal dust is the secondary phase, and the dust diffuses with air drift. With the discrete phase model turned on, the inlet and outlet boundaries are in the escape state, and the walls are in the capture state.

To simplify the numerical calculations, we make the following assumptions:

1. Dust originates entirely from the coal mining drum, ignoring coal dust falling from the coal wall.
2. The emergence rate of coal dust is 15 g/s, its minimum particle size is 10 μm , its maximum particle size is 120 μm , and it conforms to normal distribution.
3. Neglecting the effect of obstacles other than coal miners and hydraulic pillars at the working face on the flow field.

The numerical method shows good convergence, as its solution gradually approaches the true solution in each iteration. The computation of one example took about $1536 \text{ h} \times \text{core}$.

2.3. Validation

To verify the reliability of the droplet breakup model and the collision model, the particle size distribution of a single nozzle spray (spray angle, 30° ; airflow speed, 1.5 m/s) was

tested using a Malvern laser particle size analyzer (Mastersizer 3000+, Malvern Panalytical, UK) and compared with the simulation results (Figure 3). Figure 3 shows that the particle size of the droplets in the numerical simulation results is relatively large compared with the experimental test results, but in general, these two curves are very similar, confirming the reliability of the established simulation method, and the maximum error is 14%. Given the difficulty of carrying out experiments on a coal mining face, the reliability of the established simulation method was confirmed only by using the droplet size distribution data tested in the single nozzle experiment.

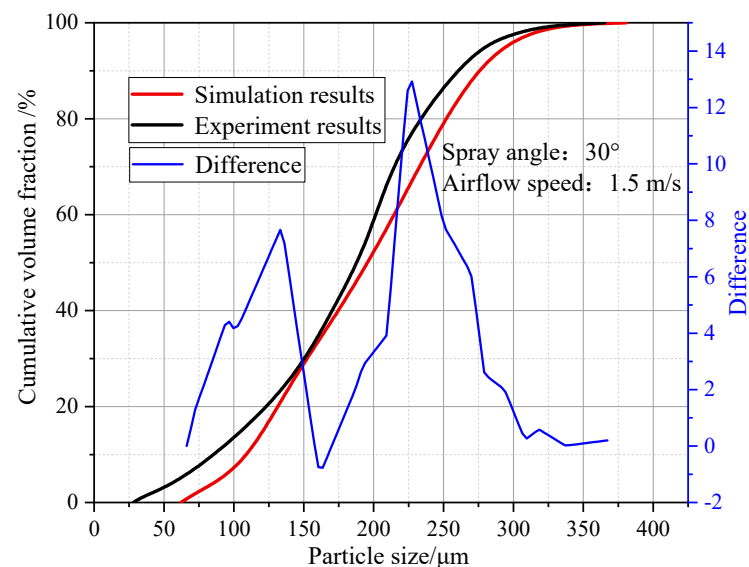


Figure 3. Comparison of droplet size distributions between simulation results and experiment data.

3. Results and Discussion

In addition to airflow speed and spray angle, many factors affect spray dust reduction. Coal dust conditions and the chemical and physical properties of the spray solution also significantly affect spray dust reduction, but airflow speed and spray angle are the easiest to adjust and thus are the most effective factors. Therefore, this study focuses on the effect of different airflow speeds and spray angles on dust reduction at a coal mining face.

3.1. The Effect of Airflow Speed on Dust Reduction

Airflow speed in coal mining faces is one of the important factors affecting spray diffusion, droplet size distribution, and dust distribution, which in turn significantly affects the spray dust reduction effect. Therefore, in this section, we first discuss the distribution characteristics of droplets in a coal mining face under different airflow conditions (1 m/s, 2 m/s, 3 m/s, and 4 m/s) and then further analyze the effect law of airflow speed on spray dust reduction.

3.1.1. Airflow Characteristics in a Coal Mining Face

Figure 4 shows the distribution of airflow speed at human breathing height (1.7 m) in a coal mining face under different airflow speed conditions. Owing to the disturbed airflow caused by the coal mining machine and the hydraulic pillar, the airflow speed distribution in the coal mining face shows the characteristics of low speed at the air inlet and air return and high speed near the coal mining machine. At the same time, a high-airflow-speed zone forms between the hydraulic strut and the coal mining machine and dilutes the dust concentration. In contrast, a low-airflow-speed zone is formed between hydraulic pillars, which is not favorable to the dilution of dust. Given the airflow speed distribution characteristics of the coal mining face, installing spray nozzles between the

hydraulic pillars and the coal mining machine, especially near the drum of the coal mining machine, achieves a better dust reduction effect.

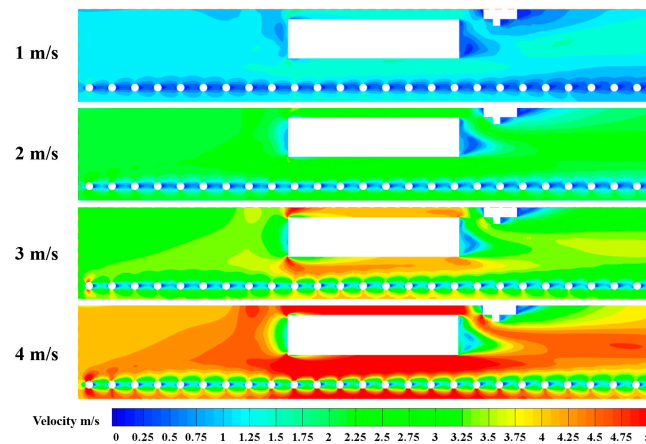


Figure 4. Airflow speed at human breathing height in coal mining face.

3.1.2. Characteristics of Droplet Distribution under Different Airflow Speeds

Three nozzles were arranged near the drum of the coal mining machine, and the direction of spraying was 30° downwind. Figure 5 shows the distribution of droplet sizes, from which it can be seen that the droplet sizes are between 50 and $300 \mu\text{m}$. Because of the coalescence effect in the droplet settling process, the overall distribution of the upper droplet size is small and the lower droplet size is large.

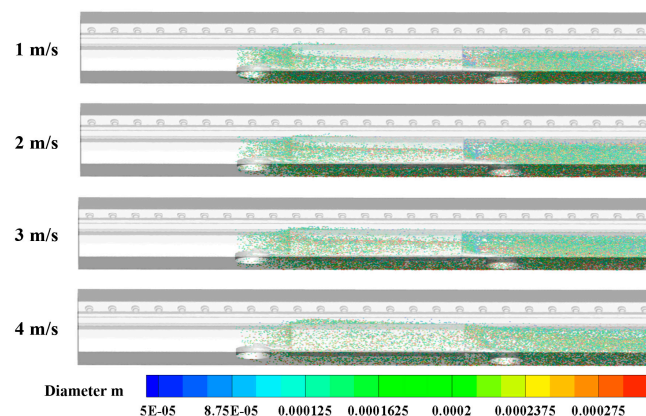


Figure 5. Size distribution of droplets in a coal mining face with different airflow speeds (3D view).

There is a significant difference in the distribution of droplets at different airflow speeds. Owing to the effect of the coal mining machine, when the airflow speed is relatively low (1 m/s , 2 m/s , or 3 m/s), a large number of droplets settle on the surface of the coal mining machine, and a droplet settlement zone is formed downstream of the nozzle position. When the airflow speed is higher (4 m/s), the droplet movement speed is larger and the settling phenomenon on the surface of the coal mining machine is weakened. Given the overall distribution, with an increase in airflow speed, the droplets settle less, but at the same time, this will also lead to less droplet distribution near the upstream coal mining machine. This suggests that the arrangement of the nozzle should fully take into account the airflow conditions of the coal mining face, and when the airflow speed is larger, the nozzles should be moved upstream appropriately.

3.1.3. Analysis of Dust Reduction Effect

The main hazard of coal dust is its threat to the health of coal miners. The actual manway is often paved with a floor that is $5\text{--}10 \text{ cm}$ high. In addition, according to

Chinese law, women are not allowed to work underground in coal mines, so all workers underground in coal mines are men in their prime. Therefore, the height of the breathing belt considered is 170 cm. Thus, we focus on dust distribution at human breathing height ($Z = 1.7$ m). At the same time, we also focus on the vertical cross section of dust distribution at the nozzle position to further analyze the isolation effect of spray on the dust. Figure 6 shows that in the absence of spray dust reduction measures, a large amount of dust can be distributed in a coal mining face, and at human breathing height, the dust will spread to the vicinity of the hydraulic pillars. Downstream of the airflow, the diffusion range of the dust exhibits an increasing trend. After taking spray dust reduction measures, the dust concentration is significantly reduced, both at human breathing height and at the spray isolation face. Arranging nozzles near the drum of the coal mining machine has a significant effect on suppressing coal dust diffusion.

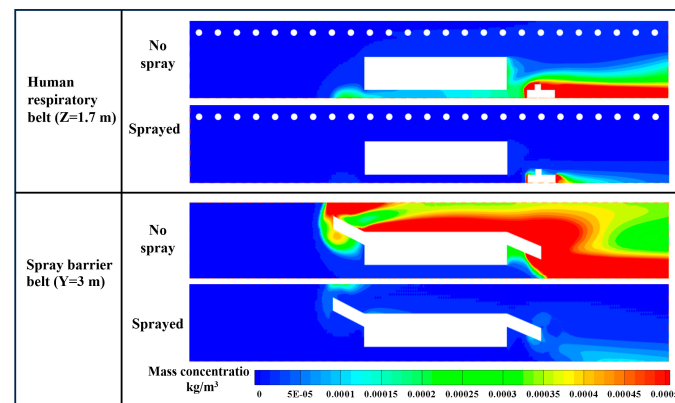


Figure 6. Effect of spraying on the distribution of dust concentration (airflow speed, 2 m/s; spray angle, 30°).

Figure 7 shows that when the spray angle is 30° , the dust concentration in the coal mining face is significantly reduced with the increased airflow speed. It should be noted that there is almost no dust near the upstream drum of the coal mining machine in Figure 6, which is because human breathing height is not on a level with the upstream drum of the coal mining machine and not because the droplets settled all of the dust. The dust distribution near the downstream drum of the coal mining machine better reflects the effect of spray dust reduction under different airflow speeds. As discussed in Section 2.1.2, as the airflow speed increases, a large number of droplets rapidly diffuse downstream and settlement on the coal miner is attenuated. On the other hand, the increase in airflow will cause a large amount of dust to rapidly diffuse downstream, which in turn dilutes the dust concentration in the vicinity of the coal miner. Thus, the dust concentration at human breathing height becomes smaller as the airflow speed increases.

In coal mining faces, the workers are usually located close to the hydraulic pillar side, with none near the coal mining machine. Therefore, if the spraying system can isolate the dust on the side of the coal mining machine and reduce its spread to the hydraulic pillar side, it can protect the staff from dust hazards. Therefore, we also focus on the isolation effect of the spray on the dust. Figure 8 illustrates the distribution of dust concentrations in the vertical cross section at the location of the nozzle under different airflow speed conditions. When the airflow speed is 1 m/s, the dust concentration in the isolation zone is high, the maximum concentration is 0.0005 kg/m^3 , and the isolation effect of the spray on the dust is very poor. With an increase in airflow speed, the isolation effect improves more and more, and when the airflow speed increases to 4 m/s, the maximum dust concentration in the isolation belt is only 0.0001 kg/m^3 .

Figure 9 shows the dust reduction efficiency of the system for a human breathing belt in the coal mining face under different airflow speed conditions. When the airflow speed is 0.5 m/s, the dust reduction effect is poor, and its rate is only about 60%. On the other

hand, an increase in airflow speed accelerates the dust diffusion, but also increases the distribution range of the spray, which in turn increases the efficiency of the spray dust reduction system. However, when the airflow speed exceeds 2 m/s, increasing the airflow speed has a limited effect on the improvement in dust reduction efficiency.

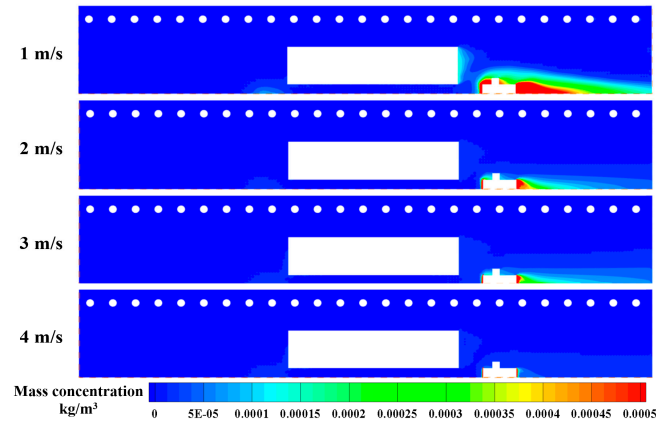


Figure 7. Distribution of dust at human breathing height under different airflow speeds (spray angle of 30° ; airflow speed of 1–4 m/s).

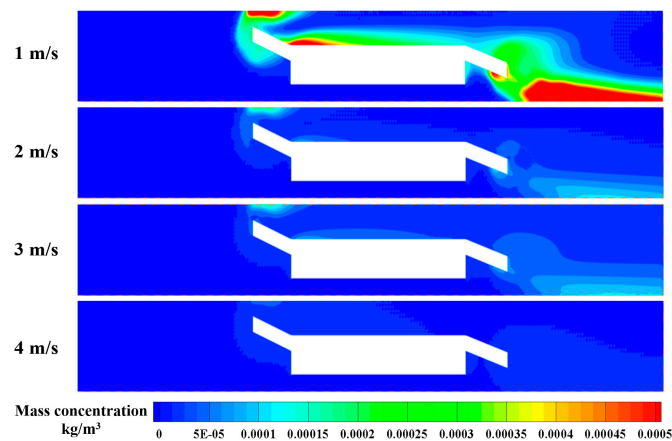


Figure 8. Distribution of dust at isolation face under different airflow speeds (spray angle of 30° ; airflow speed of 1–4 m/s).

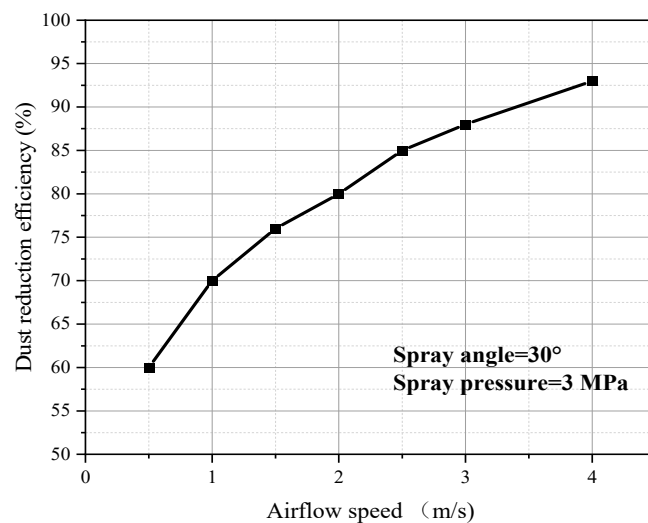


Figure 9. Dust reduction efficiency of human breathing belt at different airflow speeds (spray angle of 30°).

3.2. The Effect of Spray Angle on Dust Reduction

In addition to airflow speed, spray angle is one of the key factors in determining the effect of dust reduction via spraying. It can be adjusted according to the effect of dust reduction, whereas adjusting airflow speed is a complex operation. The spray angle determines the direction of the droplets' exit momentum, which is a key factor in determining spray diffusion characteristics. Therefore, this section focuses on the distribution characteristics of droplets and their dust reduction effects under different spray angles at an airflow speed of 1.5 m/s.

3.2.1. Characteristics of Droplet Distribution under Different Spray Angles

Figure 10 shows the particle size distributions of the droplets when the spray angle is 15°, 30°, 45°, or 60°. The change in spray angle affects droplet distribution. Figure 8 shows that when the spray angle is 15°, a large number of droplets gather near the drum of the coal mining machine, and as the spray angle increases, the droplets near the upstream drum of the coal mining machine are reduced. As the spray angle increases, the droplets' nozzle momentum direction changes, the vertically downward momentum component decreases, and the droplets are more likely to spread downstream with the airflow. This phenomenon can be more obviously seen in the distribution of droplets near the main body of the coal mining machine: when the spray angle is small, the distribution of droplets near the main body of the coal mining machine is lessened, whereas when the spray angle is larger (60°), it is greater.

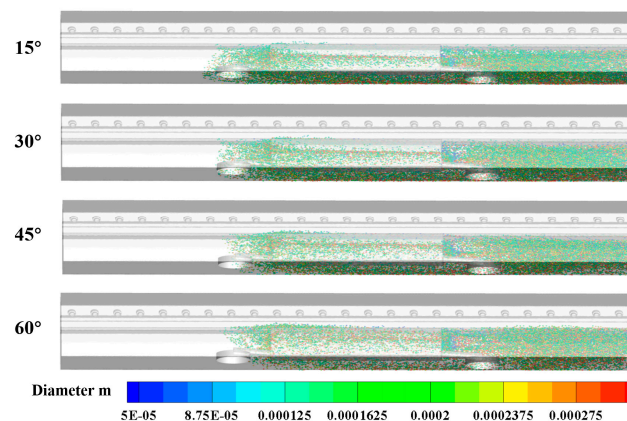


Figure 10. Size distribution of droplets in coal mining face with different spray angles (3D view).

3.2.2. Analysis of Dust Reduction Effect

Figure 11 demonstrates the distribution of dust mass concentrations at human breathing height ($Z = 1.7$ m) at spray angles of 15°, 30°, 45°, and 60°. The different heights of the two drums of the coal mining machine result in a significant difference in the dust concentration near the two drums at human breathing height. The dust near the downstream drum of the coal mining machine is mainly dominant at human breathing height. Figure 8 shows that the increase in spray angle reduces the dust concentration near the drum: when the spray angle is 45°, the spray dust reduction effect is best, and continuing to increase the spray angle is not beneficial to the effect of coal dust settlement.

Figure 12 shows the distribution of the dust mass concentration on the isolation face at different spray angles. The effect of the change in spray angle on the distribution of dust on the isolation surface is similar to that of human breathing height, i.e., with the increase in the spray angle, the dust concentration on the dust isolation surface is reduced, and when the spray angle is 45°, the spray dust reduction effect is best. Continuing to increase the spray angle is thus not beneficial to the effect of coal dust settlement. When the spray angle is too small, the nozzle momentum is mainly vertically downward, and it is difficult for the droplets to spread in the horizontal direction, resulting in poor dust reduction. When the spray angle is too large, a large number of droplets drift downstream with the airflow,

resulting in insufficient droplet concentration near the drum. When the spray angle is 45° , the droplets can spread well, both vertically and horizontally.

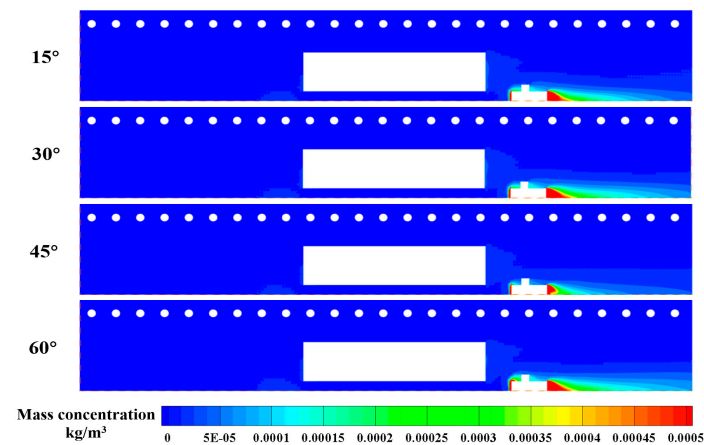


Figure 11. Distribution of dust at human breathing height under different spray angles (airflow speed of 1.5 m/s; spray angle of $15\text{--}60^\circ$).

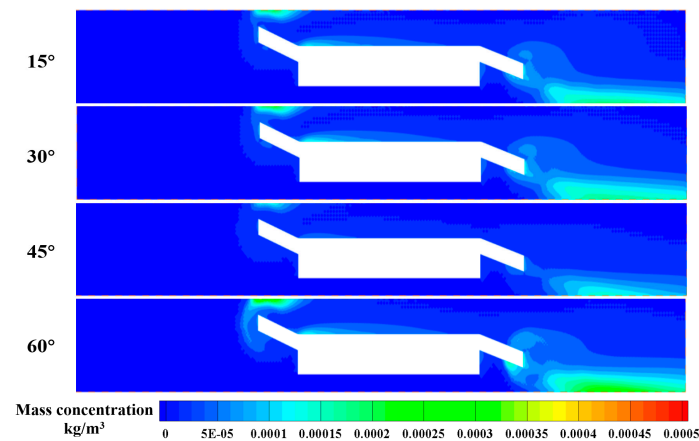


Figure 12. Distribution of dust at isolation face under different spray angles (airflow speed of 1.5 m/s; spray angle of $15\text{--}60^\circ$).

Figure 13 shows the dust reduction efficiency of the system for a human breathing belt in a coal mining face at different spray angles. When the spray angle is lower than 45° , the dust reduction efficiency increases with an increase in spray angle: when the spray angle is greater than 45° , the dust reduction efficiency decreases with an increase in spray angle. When the spray angle is 45° , the spray dust reduction effect is best, and the dust reduction efficiency reaches 82.5%.

3.3. Mathematical Modeling of Spray Dust Reduction Efficiency

According to Ma and Hou's theory [24], the amount of dust settling per unit of time and unit of volume can be expressed as:

$$\delta M = \frac{3 U_{dg} q \eta_E C A}{2 D_C \times 10^{-6}} \quad (11)$$

where U_{dg} is the relative velocity between the droplets and the wind flow, denoted as $U_{dg} = U_d + U_g$. U_d is the velocity of the droplets, m/s, and U_g is the velocity of the wind flow, m/s. In addition, q is the volume content of the droplets, i.e., $q = \frac{Q_L}{U_d A}$, where Q_L is the total volume flow rate of the droplets, m^3/s ; η_E is the dust collection efficiency of the

individual droplets; and D_C is the droplet qualitative size (for spherical droplets, we give their diameters in micrometers).

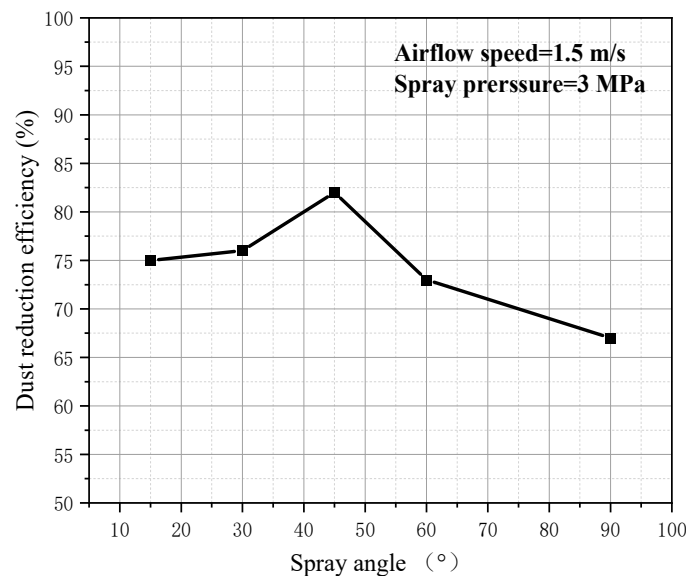


Figure 13. Dust reduction efficiency of human breathing belt at different spray angles (airflow speed of 1.5 m/s).

According to the law of conservation of mass and Equation (11),

$$-\frac{dc}{c} = \frac{3}{2} \frac{U_{dg} Q_L \eta_E}{U_g U_d A D_C \times 10^{-6}} dx \quad (12)$$

Integrating both sides provides:

$$\ln c = \frac{-3U_{dg} Q_L}{2U_g U_d A D_C \times 10^{-6}} \eta_E dx + a \quad (13)$$

Assuming that the original dust concentration is c_0 , when $x = 0$, $c = c_0$, and $a = \ln c_0$, the dust concentration, c , can be written as follows:

$$c = c_0 \exp\left(\frac{-3U_{dg} Q_L \eta_E x}{2U_g U_d A D_C \times 10^{-6}}\right) \quad (14)$$

The dust reduction efficiency, η , can be expressed as:

$$\eta = \frac{c_0 - c}{c_0} = 1 - \frac{c}{c_0} = 1 - \exp\left(\frac{-3U_{dg} Q_L \eta_E x}{2U_g U_d A D_C \times 10^{-6}}\right) \quad (15)$$

To simplify the calculation, only the inertial impact effect between dust and droplets is considered, and $1.05 \times 10^3 \text{ kg/m}^3$ is taken as the density of the coal dust particles. In addition, the cross-sectional area, A , of the roadway is 12 m^2 , the average airflow velocity of the hewing face is 1.5 m/s , and the aerodynamic viscous coefficient is $1.8 \times 10^{-5} \text{ Pa}\cdot\text{s}$. By substituting the above parameters, Equation (15) can be further simplified as [25]:

$$\eta = 1 - \exp\left[\frac{-Q_L x}{12D_C \times 10^{-6}} \left(\frac{1}{1 + \frac{0.108D_C}{D_p^2 U_d}}\right)^2\right] \quad (16)$$

Q_L is the spray flow rate, which mainly characterizes the spray velocity and spray range. Since it is difficult to accurately test droplet velocity distribution and droplet size

distribution experimentally, the spray flow rate is used to characterize the spray particle size and droplet size in general. In this study, the computational domain is considered as a whole, and therefore, the spray range is assumed to be one, with $x = 1$, and a correction factor, k , is introduced in Equation (16). In a previous study [23], the droplet size and droplet velocity in Equation (16) were ultimately expressed as expressions of the spray pressure as well, but in fact, the droplet velocity and droplet size are affected by the spray pressure and by the airflow speed and spray angle. Therefore, in this study, we focus on the influence of the spray angle and airflow speed on droplet velocity and droplet size and then establish the mathematical model of that influence on the effect of spray dust reduction. Equation (16) can be rewritten as:

$$\eta = 1 - \exp \left[\frac{-KQ_L}{D_C} \left(\frac{1}{1 + \frac{0.108D_C}{D_p^2 U_d}} \right)^2 \right] \quad (17)$$

Depending on the flow rate of a single nozzle and the number of nozzles, this can be expressed as:

$$Q_L = nQ = \frac{n\pi}{4} C_q d^2 \sqrt{\frac{2p}{\rho}} \times 10^{-3} = 4.82 \times 10^{-5} \sqrt{p} \quad (18)$$

Based on the simulation results, the following droplet sizes and droplet velocities were derived as a function of spray angle and airflow speed.

Droplet sizes (Figure 14):

$$D_C = 248.4\alpha^{-0.076} V_{air}^{-0.043} \quad (19)$$

where α is the spray angle, and V_{air} is the airflow speed.

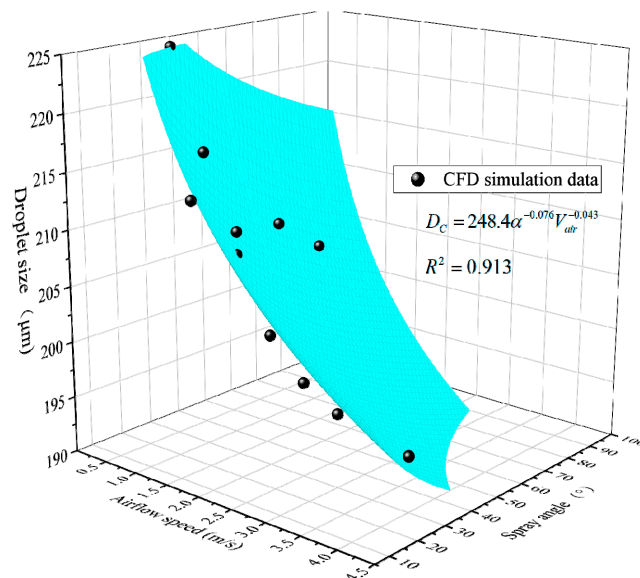


Figure 14. Correlation between droplet size and spray angle/airflow speed.

Droplet velocities (Figure 15):

$$U_d = 2.7335\alpha^{0.186} V_{air}^{0.065} \quad (20)$$

Therefore, the dust reduction efficiency can be expressed as:

$$\eta = 1 - \exp \left[\frac{-K4.82 \times 10^{-5} \sqrt{p}}{248.4\alpha^{-0.076} V_{air}^{-0.043}} \left(\frac{1}{1 + \frac{0.108 \times 248.4 \alpha^{-0.076} V_{air}^{-0.043}}{2.7335 D_p^2 \alpha^{0.186} V_{air}^{0.065}}} \right)^2 \right] \quad (21)$$

This can be simplified as:

$$\eta = 1 - \exp \left[\frac{-1.94 \times 10^{-7} K \sqrt{p}}{\alpha^{-0.076} V_{air}^{-0.043}} \left(\frac{1}{1 + \frac{9.814 \alpha^{-0.236} V_{air}^{-0.108}}{D_p^2}} \right)^2 \right] \quad (22)$$

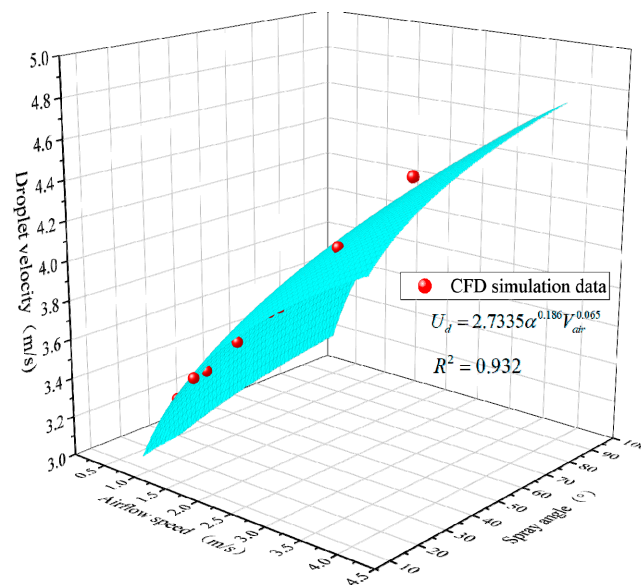


Figure 15. Correlation between droplet velocities and spray angle/airflow speed.

4. Conclusions

A numerical model that can simulate the process of droplet diffusion, dust diffusion, and droplet and dust coagulation and deposition was established, providing a new method for numerical simulation studies of spray dust reduction. Using this numerical model, the dust reduction effect of a spraying system in a coal mining face under different airflow speeds and spraying angle conditions was investigated, and the following conclusions were obtained.

1. Dust in coal mining faces mainly spreads downstream in the direction of airflow and the direction of hydraulic pillars, threatening the health of workers. Setting spraying nozzles near the dust source (the drums of the coal mining machine) can significantly reduce dust concentrations in coal mining faces from 0.0005 kg/m^3 to 0.0001 kg/m^3 .
2. An increase in airflow speed in a coal mining face increases the stagnation time of the droplets and coal dust, which provides more opportunities for the droplets to condense and settle the dust, and thus more dust settles. When the spray angle is too small, it is difficult for the droplets to spread horizontally. However, when the spray angle is too large, it will lead to an insufficient concentration of droplets near the dust source (the drums of the coal mining machine). When the spray angle is 45° , the spraying system has the best spreading range both vertically and horizontally and the best effect on dust reduction.
3. Our numerical method successfully reproduces the process of spray dust reduction and provides a tool for studying this process. In addition, based on the influence mechanism of airflow speed and spray angle on the movement of spray droplets, a

mathematical method is proposed to quickly calculate spray dust reduction efficiency, which can provide a reference value for mine dust management.

4. The numerical method proposed in this study is currently only applicable to coal dust reduction using water spray. However, it provides ideas for simulating spray dust reduction for other dust types. For other dusts without chemical reactions, its collision, aggregation, and settling patterns with water droplets are similar to those of coal dust, and the greatest differences are in the physical parameters of the dust particles. It is believed that the numerical method proposed in this manuscript can also be made applicable to other dusts by modifying the physical parameters of the dust particles.

Funding: This research was funded by the Nature Science Foundation of Chongqing (cstc2021jcyj-msxmX1153).

Data Availability Statement: Data are contained within the article.

Conflicts of Interest: The author declares that he has no known competing financial interests or personal relationships that could have appeared to influence the work reported in this paper.

References

1. Zhang, Y.; Zhang, Y.; Liu, B.; Meng, X. Prediction of the length of service at the onset of coal workers' pneumoconiosis based on neural network. *Arch. Environ. Occup. Health* **2020**, *75*, 242–250. [[CrossRef](#)] [[PubMed](#)]
2. Kurth, L.; Laney, A.S.; Blackley, D.J.; Halldin, C.N. Prevalence of spirometry-defined airflow obstruction in never-smoking working US coal miners by pneumoconiosis status. *Occup. Environ. Med.* **2020**, *77*, 265–267. [[CrossRef](#)] [[PubMed](#)]
3. Deng, J.; Li, B.; Wang, K.; Wang, C. Research status and outlook on prevention and control technology of coal fire disaster in China. *Coal Sci. Technol.* **2016**, *44*, 1–7.
4. Ding, X.; Ma, T.; Zhao, W.; Luo, Z.; Wang, T.; Sheng, Y.; Yi, X. Airborne high oil-content coal particles suppression via the electrolyte accelerated application of hydrocarbon and short-chain fluorocarbon surfactants. *Fuel* **2023**, *332*, 126192. [[CrossRef](#)]
5. Zhou, G.; Yao, J.; Wang, Q.; Tian, Y.; Sun, J. Synthesis and properties of wettability-increasing agent with multi-layer composite network structure for coal seam water injection. *Fuel* **2023**, *172*, 341–352. [[CrossRef](#)]
6. Li, J.; Zhou, F.; Li, S. Experimental study on the dust filtration performance with participation of water mist. *Process Saf. Environ. Prot.* **2017**, *109*, 357–364. [[CrossRef](#)]
7. Naiguo, W.; Wen, N.; Weimin, C.; Yanghao, L.; Liang, Z.; Lei, Z. Experiment and research of chemical de-dusting agent with spraying dust-settling. *Procedia Eng.* **2014**, *84*, 764–769. [[CrossRef](#)]
8. Dixon-Hardy, D.W.; Beyhan, S.; Goktay Ediz, I.; Erarslan, K. The use of oil refinery wastes as a dust suppression surfactant for use in mining. *Environ. Eng. Sci.* **2008**, *25*, 1189–1195. [[CrossRef](#)]
9. Ren, X.W.; Wang, M.D.; Kang, H.Z.; Lu, X.X. A new method for reducing the prevalence of pneumoconiosis among coal miners: Foam technology for dust control. *J. Occup. Environ. Hyg.* **2012**, *9*, D77–D83. [[CrossRef](#)]
10. Hu, Z.; Zhang, B.; Chang, H. A study on dust-control technology used for large mining heights based on the optimization design of a tracking spray nozzle. *Atmosphere* **2023**, *14*, 627. [[CrossRef](#)]
11. Wu, G.; Wang, P.; Liu, R.; Han, H.; Cui, Y.; Li, S. Impact of air supply pressure on the atomization characteristics and dust removal efficiency of fluid ultrasonic nozzle. *J. China Coal Soc.* **2021**, *46*, 1898–1906.
12. Nie, W.; Yi, S.; Xu, C.; Zhang, S.; Peng, H.; Ma, Q.; Guo, C.; Cha, X.; Jiang, C. Numerical simulation analysis of a combined wind-fog dust removal device in return air roadways based on an orthogonal test. *Powder Technol.* **2023**, *413*, 117890. [[CrossRef](#)]
13. Zhou, Q.; Qin, B.; Wang, F.; Wang, H.; Hou, J.; Wang, Z. Effects of droplet formation patterns on the atomization characteristics of a dust removal spray in a coal cutter. *Powder Technol.* **2019**, *344*, 570–580. [[CrossRef](#)]
14. Klima, S.S.; Reed, W.R.; Driscoll, J.S.; Mazzella, A.L. A laboratory investigation of underside shield sprays to improve dust control of longwall water spray systems. *Min. Metall. Explor.* **2021**, *38*, 593–602. [[CrossRef](#)]
15. Ren, T.; Wang, Z.; Cooper, G. CFD modelling of ventilation and dust flow behaviour above an underground bin and the design of an innovative dust mitigation system. *Tunn. Undergr. Space Technol.* **2014**, *41*, 241–254. [[CrossRef](#)]
16. Wang, P.; Wu, G.; Yuan, X.; Jiang, J.; Chen, S.; Li, S. An enhanced spray dust suppression method by micro-nano bubbles. *J. China Coal Soc.* **2022**, *47*, 4495–4503.
17. Prostański, D. Development of research work in the air-water spraying area for reduction of methane and coal dust explosion hazard as well as for dust control in the Polish mining industry. *IOP Conf. Ser. Mater. Sci. Eng.* **2018**, *427*, 12026. [[CrossRef](#)]
18. Prostański, D. Dust control with use of air-water spraying system. *Arch. Min. Sci.* **2012**, *57*, 975–990.
19. Balaga, D.; Siegmund, M.; Kalita, M.; Williamson, B.J.; Walentek, A.; Malachowski, M. Selection of operational parameters for a smart spraying system to control airborne PM10 and PM2.5 dusts in underground coal mines. *Process Saf. Environ. Prot.* **2021**, *148*, 482–494. [[CrossRef](#)]
20. Chang, S.L.; Park, S.W. An experimental and numerical study on fuel atomization characteristics of high-pressure diesel injection sprays. *Fuel* **2002**, *81*, 2417–2423.

21. Zhou, G.; Yin, W.; Feng, B. Numerical simulation on the distribution characteristics of dust-droplet field during support movement in a fully-mechanized mining face and related engineering applications. *J. China Coal Soc.* **2008**, *43*, 3425–3435.
22. ANSYS. *ANSYS Fluent Theory Guide*; ANSYS, Inc.: Canonsburg, PA, USA, 2022.
23. O'Rourke, P.J. Collective Drop Effects on Vaporizing Liquid Sprays. Ph.D. Thesis, Mechanical and Aerospace Engineering, Princeton University, Princeton, NJ, USA, 1981.
24. Ma, S.P.; Kou, Z.M. Study on mechanism of reducing dust by spray. *J. China Coal Soc.* **2005**, *30*, 297–300.
25. Wang, P.F.; Tan, X.H.; Cheng, W.M.; Guo, G.; Liu, R.H. Dust removal efficiency of high pressure atomization in underground coal mine. *Int. J. Min. Sci. Technol.* **2018**, *28*, 685–690. [[CrossRef](#)]

Disclaimer/Publisher's Note: The statements, opinions and data contained in all publications are solely those of the individual author(s) and contributor(s) and not of MDPI and/or the editor(s). MDPI and/or the editor(s) disclaim responsibility for any injury to people or property resulting from any ideas, methods, instructions or products referred to in the content.